The International Journal of Advanced Manufacturing Technology (2023) 127:1887–1894
https://doi.org/10.1007/s00170-023-11665-x

ORIGINAL ARTICLE

The influence of shielding gases on keyhole-induced porosity and nitrogen absorption in SS 304 stainless steel fiber laser welds

Hafez Khalid M.[1]

Received: 20 September 2022 / Accepted: 22 May 2023 / Published online: 2 June 2023

Abstract
Regarding porosity formation and gas content, choosing the appropriate shielding gas for laser welding is essential for achieving high-quality joints. Keyhole-induced porosity formation tendency and nitrogen content in SS 304 stainless steel welds were investigated based on the nitrogen content in shielding gases during fiber laser welding. Beads-on-plate autogenous welds were made at 5 kW continuous wave (CW) fiber laser in N_2 and Ar mixtures. Optical metallography, micro-focused X-ray, X-ray radiography, and high-speed images of the molten pool were used to investigate the porosity formation. In addition, a gas analyzer was used to study the weld metal nitrogen content. The results show that nitrogen significantly impacts the reduction of porosity in the melting zone and increases the dissolved nitrogen in the solidified weld metal, as using pure nitrogen leads to an increase in dissolved nitrogen by 36% higher than the nitrogen content in the base metal. In contrast, it has almost no significant effect on the keyhole mode.

Keywords Fiber laser · Austenitic stainless steel · Shielding gas · Porosity · Keyhole · Nitrogen content

1 Introduction

Recently, high-performance fiber laser welding has been developed; its characteristic features are deep penetration and high-speed welding compared with conventional laser welding processes [1, 2]. A thin capillary is created by high-power laser welding in the molten pool during welding, known as a keyhole. The keyhole improves energy coupling between laser beams and material, hence enhancing the absorption of laser energy and increasing penetration [3, 4]. The keyhole also represents a volatile pattern during welding. This severe instability is a critical factor in the development of weld porosities.

Porosity is one of the most severe defects in high-power laser welding because it degrades mechanical properties, particularly strength, fatigue, and elongation [1, 5–7]. Porosity in laser welding could be divided into two types, metallurgical factor-induced porosity and keyhole-induced porosity. Pores generated by low boiling point elements or surface contaminations are called metallurgical factor-induced porosities. In contrast, pores that result from deep-penetration laser welding of large-thickness components in keyhole welding mode are known as keyhole-induced porosity [8].

Shielding gases are utilized to protect the solidifying molten metal and weld keyhole from the surrounding atmosphere and hence dodge porosity and oxide inclusions, which give rise to poor weld quality. It is common knowledge that the type of shielding gases and gas flow rate in laser welding are essential and influential, not only for the protection of the weld from the encirclement air, but may have an impact on the characteristics and properties of the weld [9–11]. Besides, reactions of shielding gases with the hot metal cause changing the weld pool surface tension, providing additional energy and affecting plasma conditions, ultimately modifying the keyhole morphology and behavior during laser welding [12].

According to previous studies, the use of inert shielding gas during thick plate welding leads to the formation of many large porosities in deeply penetrated welds. In addition, active gases such as nitrogen shielding gas could be a source of porosities and brittle nitrides in carbon steel and ferritic stainless steel welds [13]. In contrast, it is often a valuable element in manufacturing austenite and duplex stainless steel alloys due to the willingness to use it as an alternative to nickel, which curtailments the

✉ Hafez Khalid M.
khalidhafez@yahoo.com

[1] Central Metallurgical Research and Development Institute (CMRDI), P.O. Box 87, Helwan, Egypt

alloying elements' costs. An important finding indicated by some studies [13, 14] is a porosity reduction in deep penetrating keyhole-type stainless steel welds by using nitrogen compared to inert gases. Due to the virtue of nitrogen's high solubility and/or high reactivity with the molten weld pool, it reduces or eliminates the gas bubbles in the weld pool, resulting in lower or even nonexistent porosity in nitrogen shielding gas than inert gases such as helium or argon. On the other hand, due to its rapid thermal cycle during the high-power laser welding process, it is assumed that nitrogen loss may be eliminated through laser welding [15].

The solubility of nitrogen in solidified weld metal of austenitic stainless steel depends on nitrogen in shielding gas, the welding temperature, and alloy composition [16, 17]. It is expected that during autogenic welding of austenitic stainless steel, the desorption and absorption of nitrogen will depend on the initial nitrogen content of the base metal and the strength of the surfactant of the weld. Arata et al. [18] indicated that gathered nitrogen from the gas-metal reactions plus the residual nitrogen from the base metal represents the total nitrogen content in the weld metal.

Conspicuously, the mechanism of nitrogen shielding gas in reducing the keyhole-induced porosity in deep penetration laser welds is unclear and needs further study. It is also necessary to clarify the nitrogen behavior in the weld pool. This study is aimed at understanding the effects of the composition of the shielding gases on the porosity content of the solidified weld metal of austenitic stainless steel and the absorbed nitrogen within it.

2 Experimental procedures

Austenitic stainless steel SS 304 plates with thicknesses of 5 mm and 8 mm were used in this study with a chemical composition that is shown in Table 1.

A continuous-wave (CW) fiber laser welding machine (IPG YLS-10000) with a maximum power of 10 kW and the beam parameter product (BPP) 4.5 mm·mrad was used to implement weld lines. Five types of shielding gas compositions were used for beads on plates laser welding at a flow rate of 40 L/min as an axial shielding gas, in which the argon/nitrogen ratios (per unit volume of the gas mixture) were 0, 0.25, 0.5, 0.75, and 1.0 respectively. Argon-nitrogen mixtures were premixed prior to welding.

A 10000 f/s framing rate high-speed camera was used to observe the molten pool behavior during welding. The porosity formation behavior during laser welding was monitored by the in situ micro-spot X-ray transmission imaging system developed by Katayama et al. [19–21]. The system uses a micro-focused X-ray source near a point source so that the minute area can be magnified and the image can be photographed. A typical example of in situ X-ray surveillance with Pt particles under 5 kW laser power-welding conditions and welding speeds of 2 m/min is shown in Fig. 1.

Subsequently, the weld lines were visually inspected and radiographically examined from the upper surface to observe the weld porosity. Hence, samples were cut out from the weld for optical observation and gas analysis. For microstructural investigation, the specimens were cut, ground, polished, and electro-etched in an oxalic acid etchant (10 g oxalic acid and 100 mL distilled water). Weld metal nitrogen

Table 1 Stainless steel SS 304 plates chemical analysis (wt.%)

Element	C	Mn	Si	S	P	Cr	Ni	Fe
%	0.05	0.98	0.62	0.004	0.028	19	8.9	Bal

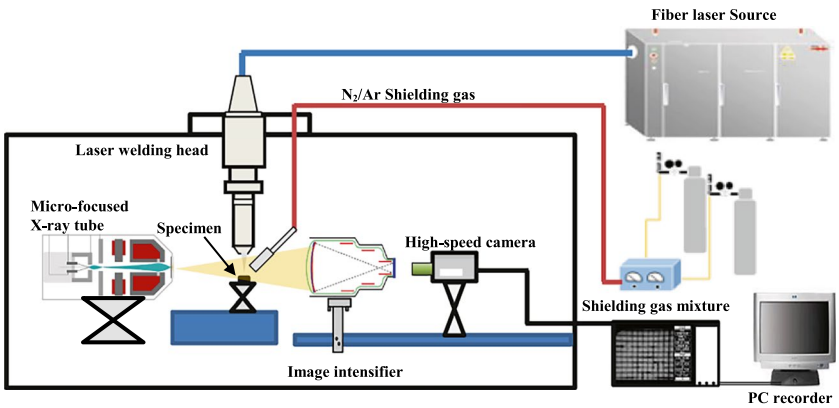

Fig. 1 Illustration of micro-focus X-ray transmission in situ surveillance system

content was analyzed using the Horiba EMGA-520 analyzer. Figure 2 shows the location of the solidified weld sample used for the nitrogen analysis.

3 Results and discussion

3.1 Monitoring of laser keyhole and keyhole-induced porosity formation

The fluctuation of the molten pool and keyhole behavior at different shielding gas ratios could be observed by a high-speed camera, as shown in Fig. 3. The high-speed camera images show that in the case of using pure argon as a shielding gas, the laser keyhole's size and shape fluctuated dramatically as can be seen in Fig. 3a. The dynamic plasma variation and the strong liquid metal flow were among the factors that contributed to the development of this phenomenon. In addition, the keyhole front is irregular in shape with the appearance of some spatter, which indicates the keyhole instability. At the same time, the situation changes when adding nitrogen, where the keyhole front becomes more stable, and if only nitrogen is used, the front of the keyhole is close to a regular oval.

The low stability of the molten pool with argon shielding gas gives the trapped gas bubbles a chance to create pores in the solidified weld metal. When nitrogen gas is used, the keyhole becomes so stable that it suppresses or prevents the formation of bubbles, thereby reducing porosity or lack of porosity.

To obtain more information regarding the keyhole behaviors at different shielding gas mixture, the inner keyhole behaviors were investigated using X-ray transmission imaging snapshots as shown in Fig. 4; welding was performed with 5 kW power and 2 m/min speed in shielding gases of 100% Ar, 50% Ar + 50% N_2, and 100% N_2, respectively. The results of monitoring X-ray transmission show the formation of a bubble near the tip of the keyhole, where, indentations in the rear keyhole wall are caused by the impact of a metallic vapor that is causing dynamic fluctuations in the tip of the keyhole. Through the interaction with the solid–liquid boundary of the bottom weld pool, the violent downward flow of liquid along the front keyhole wall generates some strong vortex flows. Consequently, a bubble forms at the tip of the keyhole due to the hydrodynamic pressure caused by the vortex flow of molten metal behind the keyhole [22] and then moved with the anticlockwise vortex to the rear part along with the molten pool bottom. Afterward, bubbles are captured by the solidification front, as the molten metal cools and solidifies due to the high solidification rate of laser welding.

In argon gas, porosity is likely to occur because the molten metal does not flow smoothly into the keyhole due to the constriction of the molten pool near the bottom of the keyhole. On the other hand, adding an active gas such

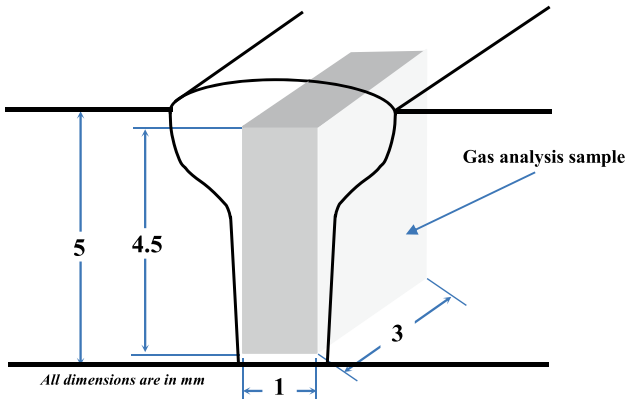

Fig. 2 Location of the gas analysis sample

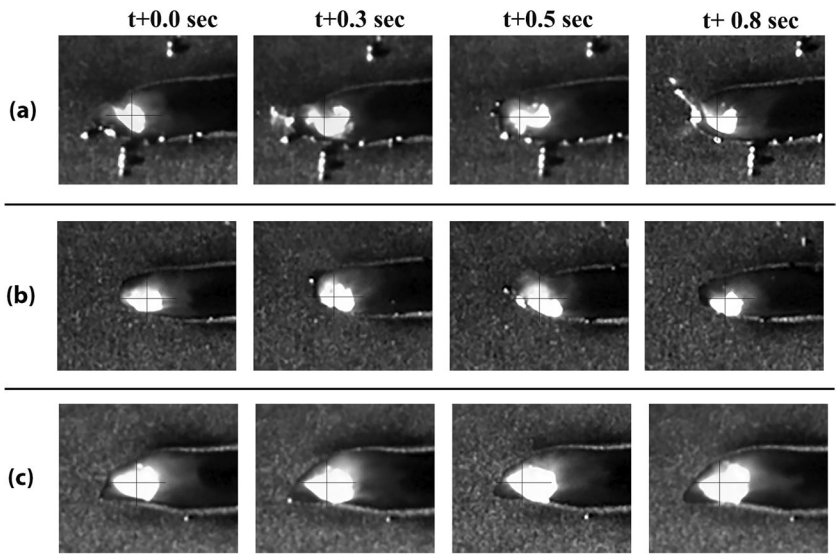

Fig. 3 High-speed photos of the molten pool at different shielding gas compassion show the keyhole formation process: **a** 100% Ar, **b** 50% Ar and 50% N_2, and **c** 100% N_2

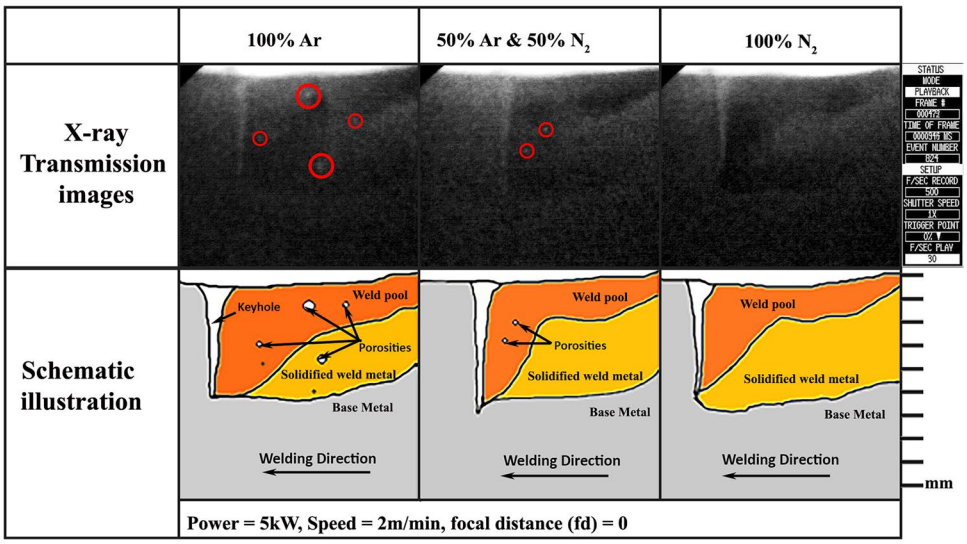

Fig. 4 Micro-focused X-ray transmission observation of keyhole behavior during 304 stainless steel fiber laser welding in different shielding gases

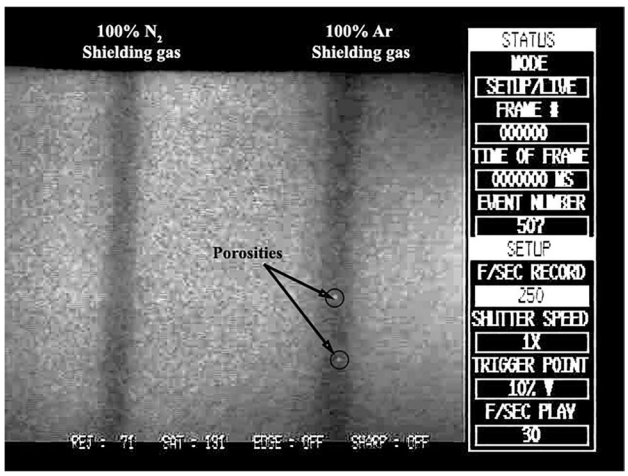

Fig. 5 X-ray inspection image of welds made using different shielding gases

as nitrogen decreases the surface tension and viscosity of the molten part. It is interpreted that the porosity is reduced because the flow of molten metal is improved by decreasing the molten metal.

Also, adding nitrogen to the shielding gases, the keyhole becomes more stable, and the number and the volume of bubbles were reduced with nitrogen increasing in the shielding gas. In the utilization case of pure nitrogen, the keyhole was stable, and no significant bubbles were formed. A radiographic test assured the previous investigation.

The results of the X-ray radiographic examination shown in Fig. 5 reveal the presence of a few pores at laser welding with argon shielding gas as well as argon with a low percentage of nitrogen, but at a higher percentage of nitrogen, pores disappeared. The analysis of cross-sections of full and partial penetration welds produced with fiber laser in various shielding gas mixtures (Fig. 6) shows a keyhole type of deep penetration.

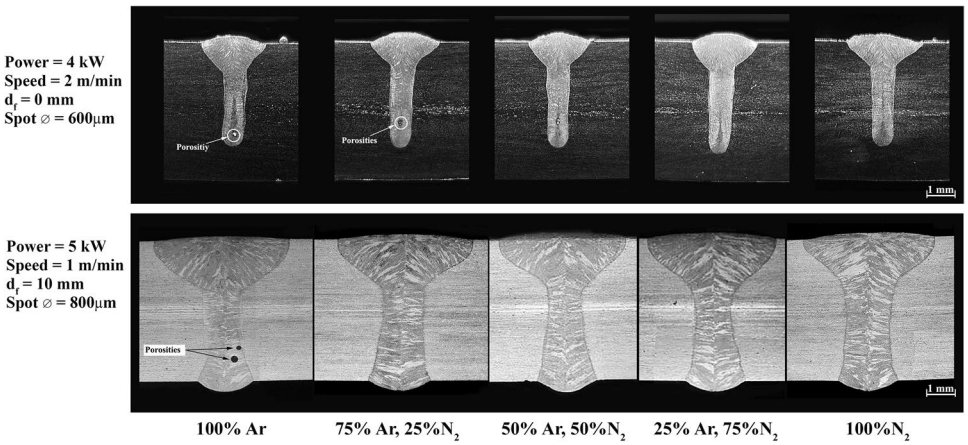

Fig. 6 Cross-sectional photos of fiber laser weld beads of type 304 stainless steel made under different welding conditions and shielding gas mixtures of argon and nitrogen

The analysis of the cross sections shows pores in the bottoms of welds that were made using a shielding gas with high levels of argon, in contrast to the welds that were made in the presence of nitrogen or high levels of it, which showed pore-free welding areas. Furthermore, the ability of austenitic stainless steel molten pools to absorb nitrogen may also contribute to the reduction in porosity when nitrogen is used [13].

3.2 Weld metal nitrogen content

As welding occurs in an open system, the partial pressure of the shielding gases approximates one atmospheric pressure = 0.1 MPa. As a result, the nitrogen partial pressure equals 0.1 MPa when nitrogen shielding is used at 100% and 0 MPa when argon shielding is used at 100%.

The nitrogen content of weld metal was measured in various samples, and the average results are represented graphically based on the partial pressure in shielding gas in Fig. 7. The results show that the measured base metal nitrogen content was 360 ppm, slightly reduced to 340 ppm when applying pure argon as a shielding gas.

Also, the results showed that an increase of nitrogen partial pressure in argon -nitrogen mixture from 0.025 MPa and more increases the N content of solidified weld metals. In the case of 0.075 MPa or more as a shielding gas, there is only a slight increase in nitrogen content. It seems to reach the solubility limit of 490 ppm in the solidified weld metal.

The laser's high temperature in the welding area leads to the dissociation of nitrogen from polyatomic molecular nitrogen gas N_2 to the monatomic nitrogen gas N [23], as shown in Eq. 1, thus facilitating the absorption of nitrogen in molten iron.

$$N_2 \text{ (shielding gas)} \Rightarrow 2N \text{ (plasma)} \Rightarrow 2N \text{ (\% weld pool)} \quad (1)$$

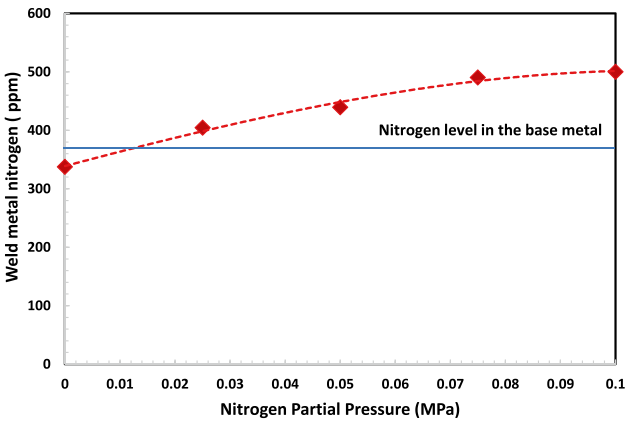

Fig. 7 SS 304 weld metal nitrogen contents for fiber laser welding with different Ar-N_2 gas ratios

At a given temperature, Sievert's law is the one that governs the equilibrium solubility of the nitrogen in the molten weld metal. According to Sievert, the concentration of nitrogen in the molten weld metal is proportional to the square root of the diatomic nitrogen partial pressure above the welding bath as indicated in Eq. 2 [24].

$$N_{eq} = K_{eq}\sqrt{P_{N_2}} \quad (2)$$

Where:

N_{eq} is the molten weld metals nitrogen concentration at equilibrium with diatomic nitrogen (wt.%)

K_{eq} is the equilibrium constant

P_{N_2} is the nitrogen Partial pressure in the shielding gases (atm).

It means that the solubility limit of nitrogen in molten stainless steel can be increased by raising the partial pressure of the diatomic gas above the melting point. Nevertheless, there are many doubts about Sievert's law's applicability when describing diatomic gas dissolution in molten weld metal in the presence of plasma. Such a plasma phase resides above the weld pool during most fusion welding processes [23–25].

Furthermore, nitrogen solubility deviates from Sieverts' law in high alloy systems, such as molten Ni–Cr or Fe–Cr. In contrast, Sievert's law is only applicable within a certain range of partial pressures of shielding gases [26].

As a further explanation of the solidified weld metal nitrogen content, it was imposed that the final nitrogen content

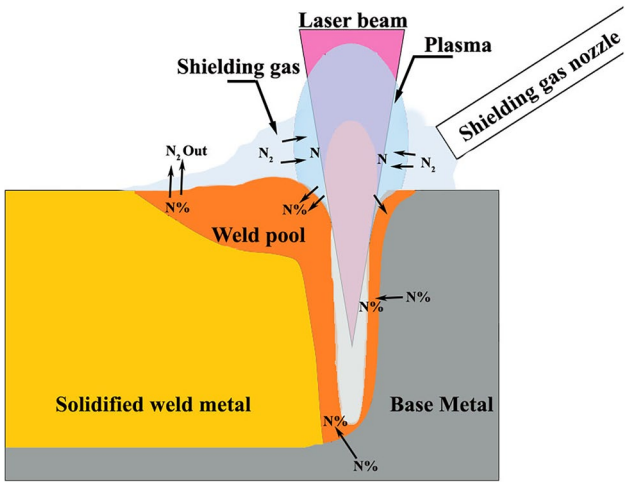

Fig. 8 Graphic illustration of the autogenous laser weld pool, showing nitrogen absorption and desorption in the weld-pool throughout fiber laser welding

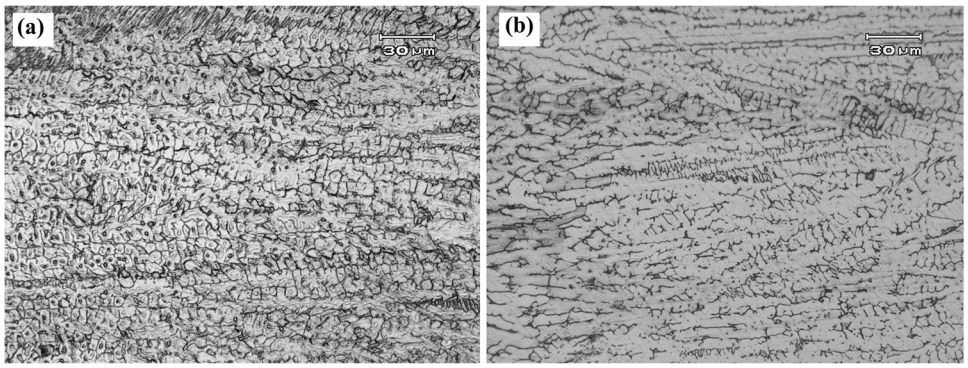

Fig. 9 Optical microscopy image of fusion line microstructure showing δ-ferrite distribution in the fusion zone of fiber laser welds made with **a** pure argon and **b** pure nitrogen

results from complex processes input and output of nitrogen atoms in the molten weld pool during laser welding.

As for the nitrogen input and absorption in the molten metal from two sources:

- Nitrogen comes from the plasma atmosphere surrounding the weld pool [27].
- Nitrogen content of the base metal is prior to melting during welding.

In addition, the process of removing dissolved nitrogen from the weld pool is done by recombining the nitrogen atoms to form nitrogen molecules (N_2) that may escape into the atmosphere, plus escaping of some atoms close to the surface during and immediately after solidification, as represented by Eq. 3.

$$2N\ (\%\ \text{weld pool}) => N_2\ (\text{gas}) \tag{3}$$

From this standpoint, increasing the turbulence of the weld pool increases the amount of escaping nitrogen due to the increase in the surface area of the weld pool. Also, the case of using only argon as a shielding gas means that there is no input of nitrogen atoms in the weld pool. It allows some of the nitrogen atoms already existing in the weld pool to combine to compose nitrogen molecules (N_2) that can get away into the surrounding atmosphere. This hypothesis is schematically illustrated in Fig. 8.

In laser welds with pure argon as the shielding gas, a significant amount of delta ferrite is observed in re-solidified fusion zones (Fig. 9a). As nitrogen is added to the shielding gas, ferrite percentages decrease. In contrast, austenite percentages increase in the fusion zone. As nitrogen is one of the storage austenite stabilizer elements, it directly affects the fusion zone ferrite content by stabilizing the austenite phase and inhibiting ferrite growth. In addition, a mathematical model has been developed for predicting the ferrite content from nickel and chromium equivalents [28]. This model is given as

$$\%Ferrite = 3[Cr_{eq} - 0.93Ni_{eq} - 6.7] \tag{4}$$

According to WRC-92 [29],

$$\text{Ni}_{\text{eq}} = \text{Ni} + 35\text{C} + 20\text{N} + 0.25\text{Cu} \tag{5}$$

$$\text{Cr}_{\text{eq}} = \text{Cr} + \text{Mo} + 0.7\text{Nb} \tag{6}$$

According to the current study, Creq was fixed at 19% while Nieq varied between 11.4 and 11.7%, depending on the nitrogen content. Hence, this is reflected in the reduction of ferrite content in the solidified weld metal.

As illustrated in Fig. 9b, the fusion zone microstructure can be observed when pure nitrogen is used as the shielding gas. Scanning electron microscopy (SEM) examination gives in-depth information on the microstructure of re-solidified fusion zones of the laser welds (Fig. 10). SEM imaging shows the

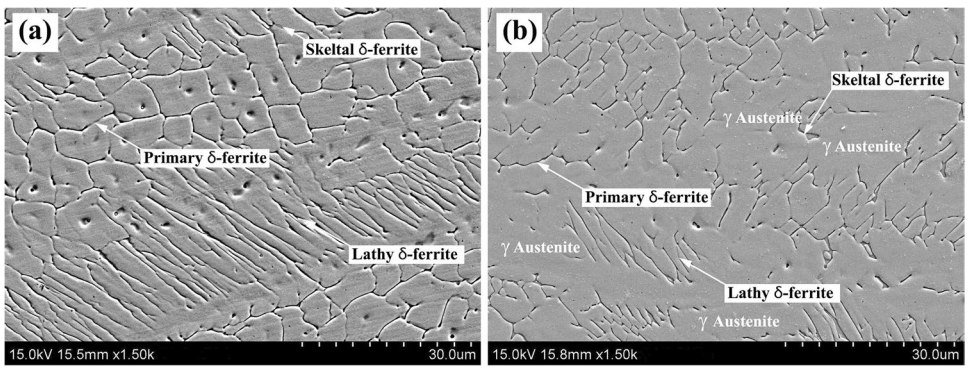

Fig. 10 SEM image of laser weld showing δ-ferrite distribution in the fusion zone of fiber laser welds made with **a** pure argon and **b** pure nitrogen

diversity in the delta ferrite such as primary delta ferrite, skeletal delta ferrite, and lathy delta ferrite in the matrix of austenite.

It is noteworthy that the researcher concluded in previous studies [2, 30] that weld metal's microstructure is significantly affected by nitrogen, as it limits the formation of delta ferrites and increases austenite. Since nitrogen is one of the storage elements of austenite, it directly affects the ferrite fusion zone content by stabilizing the austenite phase and inhibiting ferrite growth.

4 Conclusions

SS 304 stainless steel welds have been implemented at diverse mixture ratios of nitrogen-argon shielding gas by fiber laser autogenous welding.

- The mechanism of porosity formation induced by the keyhole in fiber laser welding of austenitic stainless was investigated using X-ray transmission observation. It can be summed up as follows: bubbles start from the tip of the keyhole, which increases in quantity and size in case of keyhole instability, consequently captured by the solidification front.
- An observation using a high-speed camera as well as in-situ radiography in stainless steel revealed that the high nitrogen content in shielding gases contributes to keeping the keyhole open and stable. Due to the improved keyhole stability, the keyhole did not collapse and remained open, allowing bubbles to escape from the weld pool more easily, thereby suppressing porosity. On the other hand, Nitrogen reactivity with alloying elements and/or its solubility in liquid weld pools may significantly reduce the retained porosity in unstable keyhole welds as they solidify and cool.
- The increase in nitrogen partial pressure in the shielding gas resulted in an increase in the nitrogen content of the solidified welded metal; on the other hand, the use of pure argon shielding gas decreased the nitrogen content of the solidified welded metal relative to the base metal.
- The final nitrogen content in the solidified weld metal results from a complex series of processes involving the absorption and desorption of nitrogen during fiber laser welding within the molten welds pool; it can be described using a hypothetical model. According to the proposed model, monatomic nitrogen is absorbed from the plasma atmosphere surrounding the weld pool and through nitrogen-containing base metals. Nitrogen is transported out of the weld pool by recombining the nitrogen atoms to form nitrogen molecules (N_2) that may escape into the atmosphere, plus running away of some atoms close to the surface during and immediately after solidification.
- Nitrogen significantly affects the microstructure of the re-solidified fusion zone, as it limits the formation of delta ferrites and increases austenite.

Acknowledgements The author would like to express his deepest appreciation to Prof. S. Katayama, JWRI, Osaka University, for his guidance and great wisdom, which has made this work possible. Special thanks are due to Mr. M Mizutani for his technical assistance.

Author contribution Khalid. M. Hafez conceived, designed, and executed this study and wrote the manuscript. No other person is entitled to authorship.

Funding Open access funding provided by The Science, Technology & Innovation Funding Authority (STDF) in cooperation with The Egyptian Knowledge Bank (EKB).

Data availability The data that support the findings of this study are available upon request.

Code availability Not applicable.

Declarations

Ethical approval The research meets all applicable standards concerning the ethics of experimentation and research integrity, and the following is being certified/declared authentic. The paper has been submitted with full responsibility, following the due ethical procedure, and there are no duplicate publication, fraud, plagiarism, or animal or human experimentation concerns.

Consent to participate It is not applicable because no human subjects were involved in this work.

Consent to Publish The author consents to the publication of the manuscript.

Conflict of interest The author declares no competing interests.

References

1. Katayama S, Kawahito Y, Mizutani M (2010) Elucidation of laser welding phenomena and factors affecting weld penetration and welding defects. Phys Procedia 5:9–17. https://doi.org/10.1016/j.phpro.2010.08.024
2. Hafez KM, Ghanem M, Morsy MA (2019) The influence of shielding gases on solidification structures and grain size of AISI 304 stainless steel fiber laser welds. Lasers Manuf Mater Process 6:345–355. https://doi.org/10.1007/s40516-019-00100-3

3. Kawahito Y, Matsumoto N, Abe Y, Katayama S (2011) Relationship of laser absorption to keyhole behavior in high power fiber laser welding of stainless steel and aluminum alloy. J Mater Process Technol 211:1563–1568. https://doi.org/10.1016/j.jmatprotec.2011.04.002
4. Jin X, Li L, Zhang Y (2002) A study on fresnel absorption and reflections in the keyhole in deep penetration laser welding. J Phys D Appl Phys 35:2304–2310. https://doi.org/10.1088/0022-3727/35/18/312
5. Huang B, Chen X, Pang S, Hu R (2017) A three-dimensional model of coupling dynamics of keyhole and weld pool during electron beam welding. Int J Heat Mass Transf 115:159–173. https://doi.org/10.1016/j.ijheatmasstransfer.2017.08.010
6. Li K, Lu F, Cui H et al (2015) Investigation on the effects of shielding gas on porosity in fiber laser welding of T-joint steels. Int J Adv Manuf Technol 77:1881–1888. https://doi.org/10.1007/s00170-014-6538-4
7. Xu J, Rong Y, Huang Y et al (2018) Keyhole-induced porosity formation during laser welding. J Mater Process Technol 252:720–727. https://doi.org/10.1016/j.jmatprotec.2017.10.038
8. Huang L, Hua X, Wu D, Ye Y (2019) Role of welding speed on keyhole-induced porosity formation based on experimental and numerical study in fiber laser welding of Al alloy. Int J Adv Manuf Technol 103:913–925. https://doi.org/10.1007/s00170-019-03502-x
9. Chae HB, Kim CH, Kim JH, Rhee S (2008) The effect of shielding gas composition in CO2 laser-gas metal arc hybrid welding. Proc Inst Mech Eng Part B J Eng Manuf 222:1315–1324. https://doi.org/10.1243/09544054JEM944
10. Sathiya P, Jaleel MYA (2011) Influence of shielding gas mixtures on bead profile and microstructural characteristics of super austenitic stainless steel weldments by laser welding. Int J Adv Manuf Technol 54:525–535
11. Wang H, Shi Y, Gong S, Duan A (2007) Effect of assist gas flow on the gas shielding during laser deep penetration welding. J Mater Process Technol 184:379–385. https://doi.org/10.1016/j.jmatprotec.2006.12.014
12. Quintino L, Miranda RM, Williams S, Kong CJ (2011) Gas shielding in fiber laser welding of high strength pipeline steel. Sci Technol Weld Join 16:399–404. https://doi.org/10.1179/1362171810Y.0000000002
13. Elmer JW, Vaja J, Carlton HD, Pong R (2015) The effect of Ar and N2 shielding gas on laser weld porosity in steel, stainless steels, and nickel. Weld J 94:313s–325s
14. Du TM, Pistorius PC (2003) Nitrogen control during the autogenous arc welding of stainless steel. Weld World 47:30–43. https://doi.org/10.1007/BF03266398
15. Dong W, Kokawa H, Sato YS, Tsukamoto S (2003) Nitrogen absorption by iron and stainless steels during CO_2 laser welding. Metall Mater Trans B Process Metall Mater Process Sci 34:75–82. https://doi.org/10.1007/s11663-003-0057-2
16. Cui B, Liu S, Zhang F et al (2022) Effect of welding heat input on pores in laser-arc hybrid welding of high nitrogen steel. Int J Adv Manuf Technol 119:421–434. https://doi.org/10.1007/s00170-021-08113-z
17. Dong W, Kokawa H, Tsukamoto S et al (2004) Mechanism governing nitrogen absorption by steel weld metal during laser welding. Metall Mater Trans B Process Metall Mater Process Sci 35:331–338. https://doi.org/10.1007/s11663-004-0033-5
18. Arata Y, Matsuda F, Saruwatari S (1974) Varestraint test for solidification crack susceptibility in weld metal of austenitic stainless steels. Trans JWRI 3:79–88
19. Matsunawa A, Mizutani M, Katayama S, Seto N (2003) Porosity formation mechanism and its prevention in laser welding. Weld Int 17:431–437. https://doi.org/10.1533/wint.2003.3138
20. Kawahito Y, Mizutani M, Katayama S (2007) Elucidation of high-power fibre laser welding phenomena of stainless steel and effect of factors on weld geometry. J Phys D Appl Phys 40:5854–5859. https://doi.org/10.1088/0022-3727/40/19/009
21. Gao X, Xiang J, Hafez KM, Seiji K (2013) Restoration and characteristic analysis of X-ray images of molten pool during laser deep penetration welding. Hanjie Xuebao/Trans China Weld Inst 34:1–4
22. Pang S, Chen L, Zhou J et al (2011) A three-dimensional sharp interface model for self-consistent keyhole and weld pool dynamics in deep penetration laser welding. J Phys D Appl Phys 44:25301. https://doi.org/10.1088/0022-3727/44/2/025301
23. Zhao L, Tian Z, Peng Y (2007) Porosity and nitrogen content of weld metal in laser welding of high nitrogen austenitic stainless steel. ISIJ Int 47:1772–1775. https://doi.org/10.2355/isijinternational.47.1772
24. Du Toit M, Pistorius PC (2003) Nitrogen control during the autogenous arc welding of stainless steel. Weld World 47:30–43. https://doi.org/10.1007/BF03266398
25. Katz JD, King TB (1989) The kinetics of nitrogen absorption and desorption from a plasma arc by molten iron. Metall Mater Trans B 20:175–185. https://doi.org/10.1007/BF02825598
26. Li X-Z, Li H-B, Feng H et al (2022) Nitrogen solubility in molten Ni, Ni-Cr, Ni-Mo, and Ni-Cr-Mo alloys under pressurized atmosphere. Metall Mater Trans B. https://doi.org/10.1007/s11663-022-02680-6
27. Yadaiah N, Bag S, Paul CP, Kukreja LM (2016) Influence of self-protective atmosphere in fiber laser welding of austenitic stainless steel. Int J Adv Manuf Technol 86:853–870. https://doi.org/10.1007/s00170-015-8194-8
28. Okagawa RK, Dixon RD, Olson DL (1983) The influence of nitrogen from welding on stainless steel weld metal microstructures. Weld J (Miami, Fla) 62:204s–209s
29. Kotecki DJ, Siewert TA (1992) WRC-1992 constitution diagram for stainless steel weld metals: a modification of the WRC-1988 diagram. Weld J 71:171–178
30. Hafez KM, Seiji K (2009) Fiber laser welding of AISI 304 stainless steel plates. Yosetsu Gakkai Ronbunshu/Quarterly J Japan Weld Soc 27:69–73. https://doi.org/10.2207/qjjws.27.69s